

Optical properties of bioactive europium doped hydroxyapatite (HAp:Eu³⁺)

E. ANDRONESCU^{a,b}, F. M. IORDACHE^{c,d}, C. S. CIOBANU^a, M. L. BADEA^{e,f}, A. COSTESCU^g, A. M. PRODAN^{c,d,*}

^aUniversity “Politehnica” of Bucharest, Faculty of Applied Chemistry and Materials Science, Department of Science and Engineering of Oxide Materials and Nanomaterials, 1-7 Polizu Street, P.O. Box 12-134, 011061 Bucharest, Romania

^bAcademy of Romanian Scientists (AOSR), 54 Splaiul Independentei, 050094, Bucharest, Romania

^cEmergency Hospital Floreasca, 8 Calea Floresca, Bucharest, Romania

^d“Carol Davila” University of Medicine and Pharmacy, 8 Eroii Sanitari, Bucharest, Romania

^eUniversity of Agronomic Sciences and Veterinary Medicine, 59 Mărăști Blvd., 011464, Bucharest, Romania

^fNational Institute of Materials Physics, P.O. Box MG 07, 077125, Magurele, Romania

^g“Hyperion” University of Bucharest, 169 Calea Călărașilor, 030615 Bucharest, Romania

The aim of this study was to investigate the influence of Ca_{10-x}Eu_x(PO₄)₆(OH)₂, (x_{Eu}=0; 0.05) before and after immersion in simulated body fluid (SBF) for 72 hours. The samples have been investigated by X-Ray Diffraction, FT-IR Spectroscopy, Raman Spectroscopy and Steady-State Photoluminescence. Moreover, it was studied the antibacterial activity of the powders against *Staphylococcus aureus* and *Escherichia coli* bacterial strains. Our studies revealed that after soaking in SBF solution, the average crystallite size of the samples increased. Moreover, it was noticed that the luminescence of the samples is strongly influenced by the immersion in SBF solution.

(Received July 31, 2015; accepted September 9, 2015)

Keywords: Optical properties, Europium, Simulated body fluid, Hydroxyapatite, Antimicrobial activity

1. Introduction

Recently, much attention has been paid to materials based on calcium phosphate because most of them can be used as biomaterials [1-5] and as bioactive coatings or composites [1]. These materials can be used in the medical field due to their excellent biocompatibility, their osteoconductive properties and not last but not least, due to the similarity between their chemical composition (inorganic) and the composition of bone tissue [5]. Moreover, recent studies have shown that these materials could be used for different drugs/proteins/genes delivery [6-10], in imaging or as diagnosis materials [11-14]. In addition to these medical applications, calcium phosphate based materials have many applications in industry, technology, environmental protection [15-17] and sensors [18].

One of the most studied ceramic material based on calcium phosphate is hydroxyapatite (HAp, Ca₁₀(PO₄)₆(OH)₂) [19-20]. Hydroxyapatite is the main inorganic constituent of bones and teeth [21]. In order to be able to be used in biomedical applications, HAp must possess several properties such as non-toxicity, bioactivity, biocompatibility, and it must have a good biochemical tolerance. In this context, at the moment, hydroxyapatite is being used in medicine, dentistry [22] and orthopedics [19-20]. When subjected to the human temperature and pH, HAp is a poorly soluble compound [23]. In addition, due to the above mentioned remarkable properties that hydroxyapatite possesses, many HAp based composites

and thin films have been developed with potential applications in the medical field [24].

Recent studies have shown that hydroxyapatite nanoparticles inhibit the growth of several types of cancer cells [25]. Lately, scientists have tried to obtain new particles with luminescent properties for potential applications in medical imaging and diagnosis. The hexagonal structure of hydroxyapatite allows the substitution of many types of ions (Eu, Mg, Sr, etc) without modifying its crystalline structure [15]. Thus, HAp has been doped with different ions in order to improve its physico-chemical properties [26-28].

It can be said that the interest shown recently for ionic substitutions in the hydroxyapatite structure creates the opportunity to improve the biological properties of HAp. The attributes of HAp can be enhanced by changing the structural, morphological and chemical characteristics or by exploiting the therapeutical properties of the substituting ions. Therefore, europium (Eu³⁺) doped hydroxyapatite could be used as a luminescent biological probe due to its low toxicity and stable luminescence (in the visible spectrum) [29-30]. *In vitro* (SBF media, cell testing, and antimicrobial testing) and *in vivo* (live animal tests) studies are conducted in order to test the biological properties of synthetic materials with potential biomedical applications.

Recently, several studies have been reported [30-34] which demonstrate that the biological properties (especially the antibacterial ones) of hydroxyapatite can be improved by doping it with europium ions

During *in vitro* tests, the sample was exposed to the effects of an aqueous solution (SBF) that simulates the

inorganic blood plasma in the presence or absence of cell cultures. The results of the interaction between the surface and the solution have been analyzed afterwards. Such studies have been conducted for the first time by Kokubo et al. [35]. They used SBF (simulated body fluid) in order to perform *in vitro* simulations under *in vivo* conditions.

In this paper we present the experimental results obtained for the europium doped hydroxyapatite before and after immersion in the SBF solution for 72 hours. Also, it was investigated the antibacterial activity of the obtained powders (before and after immersion in the SBF solution) against *Staphylococcus aureus* 0364 and *Escherichia coli* ATCC 25922 bacterial strains.

2. Materials and methods

2.1. Materials

In order to obtain Eu:HAp nanopowders, calcium nitrate [$\text{Ca}(\text{NO}_3)_2 \cdot 4\text{H}_2\text{O}$, Aldrich, USA], ammonium hydrogen phosphate ($(\text{NH}_4)_2\text{HPO}_4$; Alpha Aesare) and europium nitrate pentahydrate ($\text{Eu}(\text{NO}_3)_3 \cdot 5\text{H}_2\text{O}$, Alpha Aesare, Germany,) were used.

2.2. Synthesis and characterization of the samples

The synthesis method of the Eu:HAp and HAp samples was previously described [30-34]. On the other hand, the HAp-SBF and Eu:HAp-SBF samples were obtained by immersing HAp and Eu:HAp samples into SBF solution. These mixtures were maintained at body temperature and incubated for 72 hours. After incubation, the powders were removed from the SBF solution and dried at room temperature.

X-Ray Diffraction (XRD). The nanopowders were characterized by X-ray diffraction using a Bruker D8-Advance X-Ray diffractometer. The patterns were scanned in the 2θ range $20\text{--}70^\circ$.

Fourier transform infrared spectroscopy (FT-IR). The functional groups present in the prepared powders were investigated by FT-IR spectroscopy using a Spectrum BX Spectrometer. The specimens were prepared as follows: 1% of the powder was mixed and ground with 99% KBr. Tablets of 10 mm diameter were prepared by pressing the powder mixture at a load of 5 tons for 2 min. The spectra have been registered in the range of 400 to 4000 cm^{-1} with resolution 4 and 128 times scanning.

FT-Raman Spectroscopy. FT-Raman studies were performed in a backscattering geometry, under a laser excitation wavelength of 1064 nm, using a RFS 100 FT-Raman Bruker spectrophotometer.

Steady-State Photoluminescence (PL). Steady-state photoluminescence spectra have been collected from the front-face geometry of the samples with a Jobin-Yvon Fluorolog spectrometer using a xenon lamp (500 W) as an excitation source.

Antibacterial studies. The antibacterial activity of HAp, Eu:HAp, HAp-SBF, Eu:HAp-SBF was evaluated using an adapted Kirby-Bauer disk diffusion method [36]

against Gram-positive (*Staphylococcus aureus* 0364) and Gram-negative (*Escherichia coli* ATCC 25922) bacterial strains. In order to assess the antibacterial activity of the tested compounds, 1 mg of each sample was solubilized in 1 ml Dimethyl sulfoxide (DMSO) and then put on 6 mm sterile filter paper disks. The impregnated paper disks were then placed on a Mueller-Hinton (MH) agar plate previously inoculated with microbial suspensions. The susceptibility and resistance of the tested microbial strains to the investigated samples was assessed based on the presence or absence of an inhibition zone around the sterile paper disk impregnated with the tested compounds.

3. Results and discussions

Fig. 1 presents the X-ray diffraction patterns of HAp ($x_{\text{Eu}} = 0$) and Eu:HAp ($x_{\text{Eu}} = 0.05$) samples before and after being soaked in the SBF solution for 72 hours at 37°C . For all the studied samples, the X-ray diffraction patterns show a high degree of crystallinity. The diffraction peaks were identified using JCPDS card no. 9-432 and all the peaks are characteristic to the hexagonal hydroxyapatite P_{63m} space group. There were no significant difference between the XRD patterns of HAp ($x_{\text{Eu}} = 0$) and Eu:HAp ($x_{\text{Eu}} = 0.05$) samples.

The XRD patterns of pure hydroxyapatite and europium doped hydroxyapatite after being soaked in SBF for 72 hours show more intense diffraction maxima at 26 , 32 , 39.8 , 46.7 , 49.4 and 53.1° that correspond to the reflections (002), (211), (310), (222), (213) and (004) of the hexagonal hydroxyapatite.

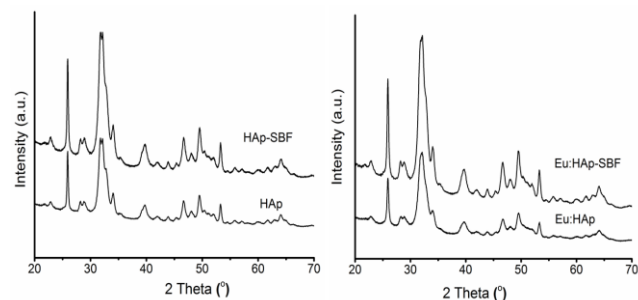


Fig. 1.- XRD spectra of HAp ($x_{\text{Eu}} = 0$) and Eu:HAp ($x_{\text{Eu}} = 0.05$) particles before and after being soaked in the SBF solution at 37°C for 72 hours (HAp-SBF and Eu:HAp-SBF)

The mean crystallite size (D) of the particles was calculated using Scherrer equation [37]:

$$D = 0.89\lambda / \beta \cos\theta$$

where λ is the wavelength, β is the full width at the half maximum of the HAp (002) line and θ is the diffraction angle. The average crystallite sizes, calculated for the HAp and Eu:HAp samples before being soaked in the SBF solution were 40.31 nm and 33.53 nm respectively. The average crystallite sizes, calculated for the samples soaked in the SBF solution (HAp-SBF and Eu:HAp-SBF) were 56.3 nm and 40.25 nm . According to the results obtained

from the XRD patterns after the immersion of HAp and Eu:HAp in SBF solution, no other phase was detectable and a decrease of crystallinity was observed.

In order to investigate the functional groups present in the obtained samples, FT-IR measurements have been performed in the transmission mode. In Figs. 2A and 2B are shown the spectra recorded for the samples containing hydroxyapatite and europium doped hydroxyapatite in the range 400–2000 cm⁻¹. Each figure is comprised of two spectra. The first figure contains the results acquired for synthetic hydroxyapatite before and after being under the influence of a certain amount of SBF, while in the second figure can be found the spectra of europium doped hydroxyapatite (Eu:HAp, $x_{Eu}=0.05$) and europium doped hydroxyapatite in stimulated body fluid (Eu:HAp-SBF, $x_{Eu}=0.05$). It can easily be observed that in both cases, the spectra of the samples containing hydroxyapatite and europium doped hydroxyapatite in SBF are smoother. Moreover, it can be noticed a broadening of the peaks, without any shifts or additional peaks. According to previous studies, it has been established that the peaks observed in all the samples correspond to the hydroxyl, phosphate and carbonate functional groups. Therefore, the peaks observed in the region 1600–1700 cm⁻¹ are associated to the H-O-H bonds present in the water lattice, while the OH functional group is highlighted by the presence of the 632 cm⁻¹ peak [27, 29].

On the other hand, previous research has concluded that the peaks found in the acquired spectra correspond to different vibrational modes associated to the PO₄³⁻ group. Therefore, the peak found at 962 cm⁻¹ is associated to the ν_1 vibration mode [30, 38], while the peaks from 475 cm⁻¹ [39], 1037 and 1097 cm⁻¹ [27, 30] are attributed to the ν_3 vibration mode. Moreover, the ν_4 vibration mode of PO₄³⁻ is highlighted by the peaks from 567 cm⁻¹ and 603 cm⁻¹ [27, 30].

Also, the peaks found in the 1400–1600 cm⁻¹ region are attributed to the ν_3 asymmetric stretching vibration of the carbonate functional group [27]. In addition, at around 870 cm⁻¹ can be found another peak attributed to the CO₃²⁻ group. However, this peak is very difficult to distinguish due to the presence of another peak present in the same region associated to the PO₄³⁻ group [27]. In previous studies, it has been concluded that the peaks present in the region from 570 cm⁻¹ to 650 cm⁻¹ are proof that the investigated samples have a well crystallized hydroxyapatite structure [38].

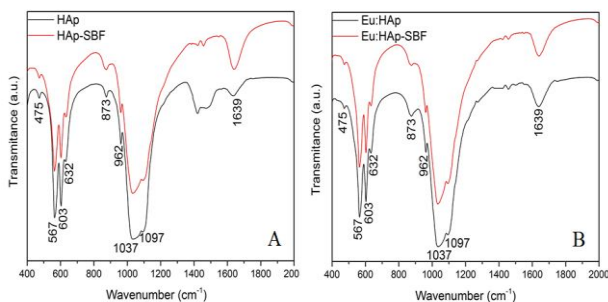


Fig. 2. FT-IR spectra of HAp ($x_{Eu} = 0$) and Eu:HAp ($x_{Eu} = 0.05$) particles before and after being soaked in SBF solution at 37 °C for 72 hours (HAp-SBF and Eu:HAp-SBF)

Complementary information to FT-IR analysis can be obtained by Raman Spectroscopy. The Raman spectra of the obtained samples are presented in the Figs. 3A and 3B. In each figure can be observed the influence that SBF has on the hydroxyapatite and europium doped hydroxyapatite respectively. After examining all the registered spectra it could be concluded that the influence of SBF on the studied samples caused a decrease of the Raman peaks intensity, no additional peaks being noticed. In all the spectra can be observed a very strong peak registered at 961 cm⁻¹ attributed to the ν_1 totally symmetric stretching mode of the tetrahedral PO₄ group, which characterizes the P-O bond [2, 26].

Moreover, the presence of the PO₄³⁻ functional group in the samples is also highlighted by the appearance in the Raman spectra of the peaks associated to the ν_2 doubly degenerated bending mode of the O-P-O bond at around 430 cm⁻¹ [2, 26, 40], to the ν_4 triply degenerated bending mode of the O-P-O bond at 590 cm⁻¹ [2, 26, 38] and to the ν_3 triply degenerated asymmetric stretching mode of the P-O bond present at 1056 and 1074 cm⁻¹ [2, 26, 40].

All the bands marked in the FT-IR and Raman spectra are characteristic to hydroxyapatite. In both cases the influence of the SBF is noticeable. In the case of FT-IR, the widening of the peaks could indicate a decrease in the crystallization of hydroxyapatite and europium doped hydroxyapatite respectively. Furthermore, the decrease of the peak intensities in the Raman spectra reinforces the conclusion that in stimulated body fluid, HAp and Eu:HAp samples are less crystalline.

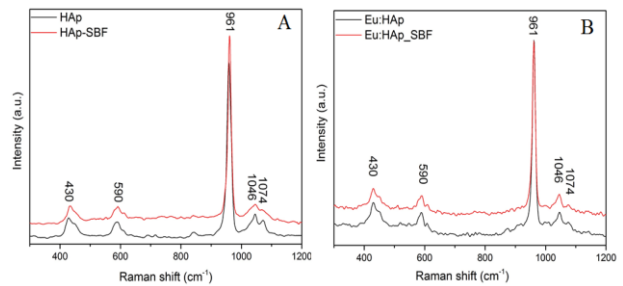


Fig. 3. Raman spectra of HAp ($x_{Eu} = 0$) and Eu:HAp ($x_{Eu} = 0.05$) powders before and after being soaked in the SBF solution at 37 °C for 72 hours (HAp-SBF and Eu:HAp-SBF)

In the emission spectra (Fig. 4) obtained for the Eu:HAp and Eu:HAp-SBF samples, three important regions can easily be distinguished: 570–582 nm mainly attributed to 5D_0 - 7F_0 transition, 582–603 nm assigned to 5D_0 - 7F_1 transition and 603–640 nm corresponding to the 5D_0 - 7F_2 transition [40–43]. All these transitions are specific to Eu³⁺ ions.

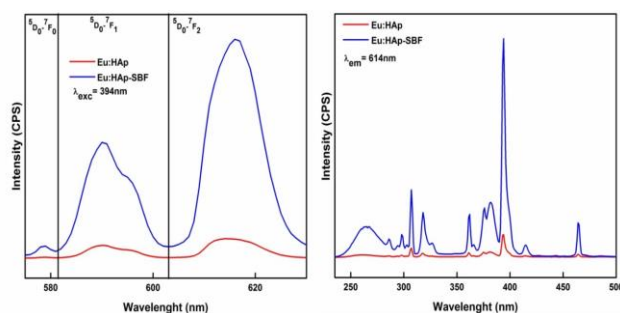


Fig. 4. Emission (left) and excitation (right) spectra of Eu:HAp ($x_{Eu} = 0.05$) powders before and after 72 hours soaking in SBF (HAp-SBF and Eu:HAp-SBF)

On the other hand, in the excitation (Fig. 4) spectra, two major peaks have been revealed: at 393 nm and 464 nm, respectively. Both maxima are wavelengths in the visible or near visible range. This property is very important in terms of biological applications because it suggests that these powders could be excited by radiation in the visible range, which would avoid damages to living cells during examinations (at the moment excitation is acquired using ultraviolet radiation, which damages the cells). It can be observed that after immersion in the SBF solution, the luminescence of the samples increased, thus showing that europium doped hydroxyapatite powders could be successfully used as drug carriers or luminescence biological probes (the emission intensity of the powders makes them easy to track and monitor by imaging techniques). The obtained results are in good agreement with the data reported in the literature [43].

The results of the qualitative screening of the antibacterial activity of Eu:HAp ($x_{Eu}=0$ and 0.05) before and after immersion in the SBF solution for 72 h are presented in Table 1.

Table 1. Results of the qualitative screening of the antibacterial activity of HAp, Eu:HAp, HAp-SBF, Eu:HAp-SBF samples against Gram-positive and Gram-negative bacterial strains

Sample	HAp	HAp-SBF	Eu:HAp	Eu:HAp-SBF.
Bacterial strains				
<i>Staphylococcus aureus</i> 0364	-	-	±	+
<i>Escherichia coli</i> ATCC 25922	-	-	±	+

The obtained results revealed that the best antibacterial activity was achieved in the case of Eu:HAp-SBF powders. Also, a good antibacterial activity was observed in the case of Eu:HAp sample. For the powders with $x_{Eu}=0$ (HAp and HAp-SBF) no antibacterial activity was noticed [30-34]. We can conclude that the presence of

the Europium in the samples increases the antibacterial activity of the HAp samples. On the other hand, it was observed that the antibacterial activity of the Eu:HAp is slightly influenced by the immersion in the SBF solution.

4. Conclusions

After immersion in SBF solution for 72 h, the average crystallite size increased for both samples (HAp-SBF and Eu:HAp-SBF). FT-IR investigations of europium doped hydroxyapatite before and after immersion in SBF did not show any change in the crystal structure of the hydroxyapatite. The FT-IR spectra of EuHAp and Eu:HAp-SBF did not present any additional bands associated to other calcium phosphate phases which would be expected for partially transformed HAp. FT-IR and Raman studies indicate a decrease in the crystallinity of hydroxyapatite and europium doped hydroxyapatite, after being immersed in SBF for 72 h, in agreement with the XRD studies. The europium doped hydroxyapatite powders immersed in SBF solution exhibited a better antimicrobial activity compared to Eu:HAp powders. The PL studies revealed that after immersion in the SBF solution, the luminescence of the samples increased. Their improved luminescence along with their antibacterial activity obtained after the immersion in the SBF suggest that europium doped hydroxyapatite powders could be successfully used as drug carrier or luminescent biological probe.

Acknowledgements

This work was financially supported by the Sectoral Operational Programme Human Resources Development 2007-2013 of the Ministry of European Funds through the Financial Agreement POSDRU/159/1.5/S/134398. The antimicrobial studies were financially supported by the PN-II- 259/01/07/2014 funded by the Ministry of Education - UEFISCDI.

References

- [1] M. Valletregi, Prog. Solid State Chem. **32**, 1 (2004).
- [2] S. Koutsopoulos, J. Biomed. Mater. Res. **62**, 600 (2002).
- [3] L. Xia, K. Lin, X. Jiang, Y. Xu, M. Zhang, J. Chang, Z. Zhang, J. Mater. Chem. B **1**, 5403 (2013).
- [4] M. Bohner, S. Tadier, N. Garderen, A. Gasparo, N. Dobelin, G. Baroud, Biomater. **3**, e25103 (2013).
- [5] S. Dorozhkin, Materials, **2**, 1975 (2009).
- [6] N. Niu, D. Wang, S. Huang, C. Li, F. He, S. Gai, X. Li, P. Yang, Cryst. Eng. Comm. **14**, 1744 (2012).
- [7] Y.-P. Guo, Y.-B. Yao, Y.-J. Guo, C.-Q. Ning, Microporous Mesoporous Mater. **155**, 245 (2012).
- [8] V. Uskokovic, D. P. Uskokovic, J. Biomed. Mater. Res. **96B**, 152 (2011).
- [9] C. Zhang, C. Li, S. Huang, Z. Hou, Z. Cheng, P.

- Yang, C. Peng, J. Lin, *Biomaterials* **31**, 3374 (2010).
- [10] F. Ye, H. Guo, H. Zhang, X. He, *Acta Biomater.* **6**, 2212 (2010).
- [11] E. I. Altinoglu, T.J. Russin, J.M. Kaiser, B.M. Barth, P. C. Eklund, M. Kester, James. H. Adair, *ACS Nano* **2**, 2075 (2008).
- [12] D. E. Wagner, K. M. Eisenmann, A. L. Nestor-Kalinoski, S. B. Bhaduri, *Acta Biomater.* **9**, 8422 (2013).
- [13] F. Chen, P. Huang, Y. J. Zhu, J. Wu, D. X. Cui, *Biomaterials* **33**, 6447 (2012).
- [14] A. Ashokan, G. S. Gowd, V. H. Somasundaram, A. Bhupathi, R. Peethambaran, A. K. Unni, S. Palaniswamy, S. V. Nair, M. Koyakutty, *Biomaterials* **34**, 7143 (2013).
- [15] M. Vukomanovic, Z. Vojka, M. Otonicar, U. Repnik, B. Turk, S. D. Skapina, D. Suvorova, *J. Mater. Chem.* **22**, 10571 (2012).
- [16] H. Sun, F. Z. Su, J. Ni, Y. Cao, H. Y. He, K. N. Fan, *Angew Chem.* **48**, 4390 (2009).
- [17] J. Oliva, J. Cama, J. L. Cortina, C. Ayora, J. De Pablo, *J. Hazard Mater.* **213–214**, 7 (2012).
- [18] Y. Zhang, Y. Liu, X. Ji, C.E. Banks, W. Zhang, *J. Mater. Chem.* **21**, 14428 (2011).
- [19] T. Kokubo, *Bioceramics and Their Clinical Applications*, CRC Press, Boca Raton (2008).
- [20] S. V. Dorozhkin, *Calcium orthophosphates: applications in nature, biology and medicine*, Pan Stanford, Singapore (2012).
- [21] S. Weiner, H. D. Wagner, *Annu. Rev. Mater. Sci.* **28**, 271 (1998).
- [22] S. V. Dorozhkin, M. Epple, *Angew. Chem. Int. Ed. Engl.* **41**, 3130 (2002).
- [23] Z. F. Chena, B. W. Darvell, V. W. H. Leung, *Arch. Oral. Biol.* **49**, 359 (2004).
- [24] A. Sarkar, S. Kannan, *Ceram. Int.* **40**, 6453 (2014).
- [25] C. H. Hou, S. M. Hou, Y. S. Hsueh, J. Lin, H. C. Wu, F. H. Lin, *Biomaterials*, **30**, 3956 (2009).
- [26] P. N. de Aza, F. Guitian, C. Santos, S. de Aza, R. Cusco, L. Artus, *Chem. Mater.* **9**, 916 (1997).
- [27] C. S. Ciobanu, C. L. Popa, D. Predoi, *J. Nanomater.* **2014**, 1 (2014).
- [28] C. S. Ciobanu, F. Massuyeau, L. V. Constantin, D. Predoi, *Nanoscale Res. Lett.* **6(1)**, 613 (2011).
- [29] C. S. Ciobanu, S. L. Iconaru, F. Massuyeau, L. V. Constantin, A. Costescu, D. Predoi, *J. Nanomater.* **2012**, 1 (2012).
- [30] C. S. Ciobanu, E. Andronescu, B. S. Vasile, C. M. Valsangiacom, R. V. Ghita, D. Predoi, *Optoelectron Adv. Mater- Rapid Comm.*, **4**, 1515 (2010).
- [31] S. L. Iconaru, M. Motelica-Heino, D. Predoi, *J. Spectrosc.* **2013**, 1 (2013).
- [32] C. S. Ciobanu, S. L. Iconaru, F. Massuyeau, L. V. Constantin, A. Costescu, D. Predoi, *J. Nanomater.* **2012**, 1 (2012).
- [33] C. S. Ciobanu, F. Massuyeau, E. Andronescu, M. S. Stan, A. Dinischiotu, D. Predoi, *Dig. J. Nanomater. Bios.* **6**, 1639 (2011).
- [34] C. L. Popa, C. S. Ciobanu, S. L. Iconaru, M. Stan, A. Dinischiotu, C. C. Negrila, M. Motelica-eino, R. Guegan, D. Predoi, *Cent. Eur. J. Chem.* **12**, 1032 (2014).
- [35] T. Kokubo, H. Kushitani, S. Sakka, T. Kitsugi, T. Yamamuro, *J. Biomed. Mater. Res.* **24**, 721 (1990).
- [36] J. H. Jorgensen, J. D. Turnidge, *Susceptibility test methods: dilution and disk diffusion methods. Manual of Clinical Microbiology*, American Society for Microbiology, Washington (2003).
- [37] R. Murugan, S. Ramakrishna, *Cryst. Growth Des.* **5**, 111 (2005).
- [38] M. Markovic, B. O. Fowler, M. S. Tung, *J. Res. Natl. Inst. Stand. Technol.* **109**, 553 (2004).
- [39] C. S. Ciobanu, S. L. Iconaru, C. L. Popa, M. Motelica-Heino, D. Predoi, *J. Nanomater.* **2015**, 1 (2015).
- [40] G. R. Sauer, W. B. Zunic, J. R. Durig, R. E. Wuthier, *Calcif. Tissue Int.* **54**, 414 (1994).
- [41] A. Doat, F. Pellé, N. Gardant, A. Lebugle, *J. Solid State Chem.* **177**, 1179 (2004).
- [42] M. Long, F. Hong, W. Li, F. Li, H. Zhao, Y. Lv, H. Li, F. Hu, L. Sun, C. Yan, Z. Wei, *J. Lumin.* **128**, 428 (2008).
- [43] A. Sepahvandia, F. Moztarzadeha, M. Mozafaria, M. Ghaffaria, N. Raeeb, *Colloids Surf. B* **86**, 390 (2011).

*Corresponding author: prodan1084@gmail.com